Blends of a 3-Miktoarm Star Terpolymer (3μ-ISD) of Isoprene (I), Styrene (S), and Dimethylsiloxane (D) with PS and PDMS. Effect on Microdomain Morphology and Grain Size

Kazuhiro Yamauchi, Satoshi Akasaka, and Hirokazu Hasegawa*

Department of Polymer Chemistry, Graduate School of Engineering, Kyoto University, Katsura, Nishikyo-ku, Kyoto 615-8510, Japan

Hermis Iatrou and Nikos Hadjichristidis*

Chemistry Department, University of Athens, Panepistimiopolis, Zografou 15771, Athens, Greece

Received April 6, 2005; Revised Manuscript Received July 17, 2005

ABSTRACT: The morphologies of a 3-miktoarm star terpolymer of isoprene (I), styrene (S), and dimethylsiloxane (D), 3μ-ISD, and its blends with PDMS and PS homopolymers, having a lower molecular weight than the corresponding blocks of the star, were studied. Combined EF-TEM and 3D electron tomography clearly revealed that three kinds of cylindrical structures, composed of three different blocks, joined to fill the space and that these cylinders were curved collectively into an arc. The grain size of this star terpolymer was extremely small compared with that of other known linear block copolymers. By blending the neat 3μ-ISD with a small quantity of PDMS homopolymer (5 wt %), the morphology remained the same, but the grain size increased dramatically. It seems that the PDMS homopolymer inserts into the PDMS phase of the star terpolymer and straightens the bent cylinders, thereby increasing long-range order. However, the extra PDMS accumulates in line defects, which if controlled could be beneficial as waveguides in photonic crystals. Blending with PS leads to smaller grain sizes and unstable hexagonal symmetry, which disappears upon the addition of extra PS. Therefore, tetragonal symmetry is inherent in the neat star.

1. Introduction

Thanks to the recent advances in polymer synthesis, well-defined block copolymers with more than two different blocks have been prepared. Some examples include linear ABC triblock terpolymers (l-ABC), 3-miktoarm star terpolymers (3μ-ABC), and linear ABCD tetrablock quaterpolymers (l-ABCD). Morphological studies of these multiblock, multicomponent copolymers, MMCPs, revealed novel microdomain morphologies that depend not only on the chemistry but also on the macromolecular architecture (l-ABC,[1−16] 3μ-ABC,[17−22] and l-ABCD[23,24]). For example, whereas l-ABC would have both junction points residing on surfaces, 3μ-ABC would have the single junction residing on a line. This difference in the spatial arrangement of the junction points will dramatically change the self-assembly and consequently the resulting microdomain structures. Dotera et al. investigated the morphology of 3μ-ABC with an arm-length ratio of 1:1:x (x: variable) by a computer simulation method and predicted that all three components would form polygonal cylindrical microdomains with the junction points confined to one line.[25,26] Experimental evidence corroborates Dotera's predictions. Such characteristic morphologies for 3μ-ABC have not been found for l-ABCs.

Historically, block copolymers have found applications as thermoplastic elastomers, adhesives, and compatibilizers for polymer blends.[27−29] In the last 10 years, however, an enormous research effort has indicated that block copolymers will play a significant role in nanotechnology (e.g., as photonic crystals[30] or high-density information storage media[31,32]). For instance, self-assembling nanopatterns created by block copolymers can be applied as masks for the top-down lithographic method. Along these lines, regularly packed cylindrical structures are one of the favorable patterns, as long as they are arranged perpendicularly to the surface. Cylindrical arrangements differ between linear block copolymers and miktoarm stars. Linear block copolymers have either single or multicoaxial cylinders embedded in a matrix, whereas miktoarm stars form polygonal columns without a matrix. These multicoaxial cylinders as well as the polygonal columns will certainly increase the potential applications of block copolymers in nanotechnology.

To adopt block copolymers as functional nanomaterials (e.g., lithographic masks), it is necessary to control the size of the grains, making them as large as possible. In general, random nucleation of microdomain structures in block copolymers results in polygrain structures with different orientations. Therefore, the development of methods for aligning such grains into a macroscopically anisotropic single-crystal-like structure is critical. Successful control of the microdomain structures of linear block copolymers was achieved by applying an electric[38]/magnetic field[39] as well as shear flow[40,41] or a temperature gradient.[42,43] There has been no report, to our knowledge, concerning the alignment in 3μ-ABCs. Because the difference in grain size between linear and star ABCs is so great,[22] the orientation alignment methods given above cannot be applied satisfactorily to the stars. Thus, the small grain problem associated with the stars must be examined, and another method for increasing grain size must be developed.

In our previous study,[22] the microdomain structure of an ABC 3-miktoarm star terpolymer consisting of

* Corresponding authors. E-mail: hasegawa@alloy.polym.kyoto-u.ac.jp.

10.1021/ma050716k CCC: $30.25
Published on Web 08/18/2005

Table 1. Characteristics of the 3-Miktoarm Star Terpolymer (3μ-ISD) and Its Blends with PDMS (3μ-ABC-D) and the PS Homopolymers (3μ-ABC-S)

sample	3μ-ISD (wt %)	homoPDMS (D) or homoPS(S) (wt %)	volume ratio of PI/PS/PDMS
3μ-ISD	100	0	1.00:0.80:0.84
3μ-ISD-2D	95	5	1.00:0.80:0.99
3μ-ISD-3D	87.5	12.5	1.00:0.80:1.23
3μ-ISD-4D	78.3	21.7	1.00:0.80:2.00
3μ-ISD-5S	93.8	6.2	1.00:1.00:0.84
3μ-ISD-6S	87.5	12.5	1.00:1.13:0.84
3μ-ISD-7S	79.6	20.4	1.00:1.46:0.84

polyisoprene (PI, 20.7 kg mol^{-1}), polystyrene (PS, 19.5 kg mol^{-1}), and poly(dimethylsiloxane) (PDMS, 19.0 kg mol^{-1}), 3μ-ISD, was investigated by energy-filtering transmission electron microscopy (EF-TEM) and electron tomography. Electron tomography revealed that three kinds of cylindrical microdomain structures are adjoined to fill the space and that these cylindrical domains were curved collectively into an arc. We concluded that the interplay between the asymmetric interactions among the three components of the terpolymer and their asymmetric volume fractions created the tension, resulting in bent cylinders. Moreover, this may be the reason that long-range order is missing, resulting in an extremely small grain size in 3μ-ISD. To resolve the problem of the small 3μ-ISD grain size, we investigated the effect of the asymmetric volume fraction by blending the star with PS or PDMS having a lower molecular weight than the corresponding block. This approach proved to be faster and simpler than the tedious and time-consuming synthesis of new 3μ-ABCs with different compositions.

2. Experimental Section

The synthesis of 3μ-ISD (PI: 20.7 kg mol^{-1}; PS: 19.5 kg mol^{-1}; PDMS: 19.0 kg mol^{-1}) was based, on one hand, on the controlled anionic polymerization of hexamethylcyclotrisiloxane and, on the other hand, on the selective replacement of the chlorines of trichloromethylsilane by living chains of polyisoprene, PI, polystyrene, PS, and poly(dimethylsiloxane), PDMS. The linking reaction was monitored by size-exclusion chromatography (SEC), and the final product was fractionated to purify the star polymer. The good agreement between the determined PS, PI, and PDMS contents (^{1}H NMR and UV) and those calculated indicates high degrees of molecular and compositional homogeneity. This is also supported by the narrow molecular weight and compositional distribution of the final star obtained by SEC. Details of the synthesis are described elsewhere.[44] For blending purposes, low-molecular-weight PS (M_n = 2.8 kg mol^{-1}, M_w/M_n = 1.05) and PDMS homopolymer (M_n = 1.3 kg mol^{-1}, M_w/M_n = 1.02) were employed (Table 1).

The film specimens were prepared in a Petri dish by casting from a 7 wt % polymer solution in toluene. The solvent was slowly evaporated over several weeks at room temperature, followed by annealing at 150 °C for 12 h in a vacuum oven. The three components, PS, PI, and PDMS, in 3μ-ISD with each molecular weight of ca. 20 kg mol^{-1} are considered to be strongly segregated at this annealing temperature. The film specimens were subsequently ultramicrotomed with a diamond knife under dry conditions at −120 °C using a Reichert ultracut E ultramicrotome equipped with a cryogenic sectioning unit prior to staining. The ultrathin sections were stained with the vapor of a 2 wt % aqueous solution of osmium tetraoxide (OsO_4) at room temperature for 1 h. The morphology of the blends was observed with a transmission electron microscope (JEM-2000FX, JEOL Co., Ltd.) at an acceleration voltage of 160 kV, and the neat 3μ-ISD sample was examined under a JEOL JEM-2010FEF energy-filtering transmission electron microscope equipped with an omega filter for the precise analysis of the microdomain compositions.

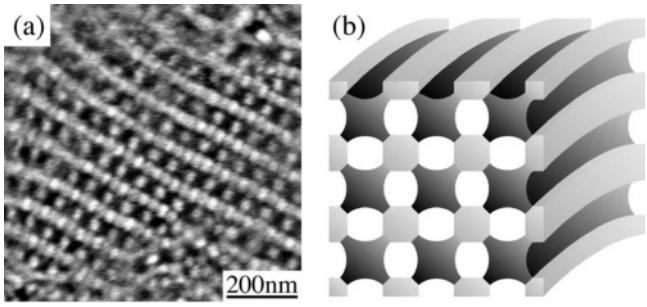

Figure 1. (a) Zero-loss image of 3μ-ABC stained with OsO_4. (b) Schematic illustration of the model for the microdomain structure of 3μ-ISD consisting of dark (PI), gray (PDMS), and bright (PS) cylinders with a characteristic shape (St. Andrew's cross).

3. Results and Discussion

For purposes of comparison and clarity, we include here a short summary of the most pertinent results already reported in our previous work[22] concerning the morphological analysis of neat 3μ-ISD. The zero-loss image (ΔE = 0 eV) obtained by EF-TEM of the OsO_4-stained ultrathin section of neat 3μ-ISD is given in Figure 1. The darkest area corresponds to the PI microdomains (containing Os atoms), the less-dark area corresponds to the PDMS microdomains containing Si atoms, and the brightest area corresponds to the PS. The contrast, however, between the PS and PDMS microdomains is too low to distinguish between the two microphases (Figure 1a). Consequently, the only discernible region corresponds to PI (Figure 1a). To distinguish the other two phases, we carried out EF-TEM experiments at ΔE = 110 and 230 eV, with the details described elsewhere.[22,45] Careful analysis of the images revealed the one-to-one correspondence between the three microdomains observed in the TEM and the three 3μ-ISD components, as indicated in Figure 1b.

Electron tomography of the OsO_4-stained neat specimen indicated that the PI microdomain has a bent-cylindrical shape aligned in a tetragonal array. The PDMS microdomains were also shown to form a bent-cylindrical structure aligned in a tetragonal array in the 3D image obtained by electron tomography of the unstained specimen in which only PDMS domains containing Si atoms are visible. Inevitably, the remaining PS microdomains should also be bent cylinders. This characteristic bending is probably a consequence of confining the central junction points of 3μ-ISD on arched lines where the three interfaces meet (Figure 1b).

The lower-magnification image of Figure 1a is shown in Figure 2. The square area marked in the Figure corresponds to the image in Figure 1a. Although the grain with the structural regularity shown in Figure 1a is the largest of all of our TEM observations, its size is only ca. 500 nm, which is extremely small compared with those commonly observed for linear block copolymers. In general, block copolymers exhibit continuous grains having different orientations, whereas, curiously, 3μ-ISD exhibits small, discrete St. Andrew's grains in large matrixes without microdomain regularity, where the three phases in the matrixes are not distinguishable, even after annealing. The irregular matrix surrounding the St. Andrew's islands cannot be the result of contamination either by linear impurities or by the annealing or microtoming process but must be inherent to the

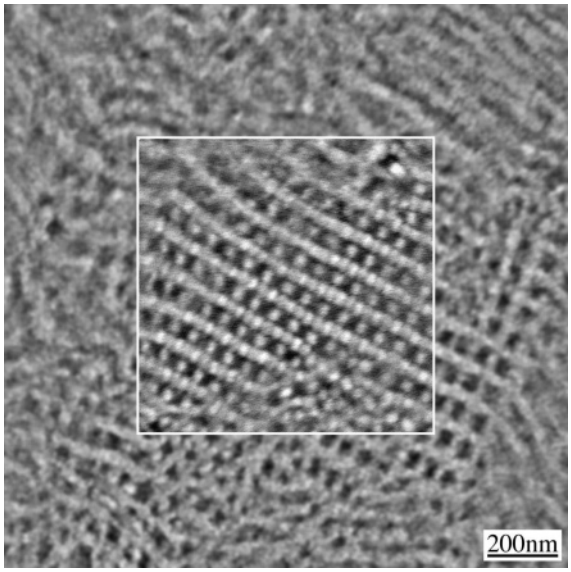

Figure 2. Low-magnification TEM image of 3μ-ISD stained with OsO_4. The square area outlined in white corresponds to the image in Figure 1a.

material. GPC measurements rule out the possibility of contamination, and the experimental procedures prevent the disruption of the regular domains.

Block copolymer samples for microdomain−structure observations are generally prepared by a solution-casting method that greatly influences the resulting morphology, which is often not an equilibrium one. This cast morphology preserves the "memory" of the structure present in the solution at that particular concentration because upon evaporation of the solvent the morphology is frozen by the vitrification of the least-soluble chain.[46] The excessively irregular microdomain structure in 3μ-ISD could be a nonequilibrium one frozen before a regular structure is organized. To remove the "memory" of the solution-casting process, cast films are commonly treated thermally. 3μ-ISD was annealed at 150 °C for 12 h without any improvement in regularity. Further annealing of the specimen at 150 °C for 1 week did not improve the regularity either. Such an irregular microdomain structure, even after annealing, cannot be considered to be the equilibrium structure. Therefore, thermal treatment should not be considered to be effective for 3μ-ISD. To obtain large grains of the regular microdomain structure in 3μ-ISD, it is essential to ensure that the grain size of the regular microdomain structure in the as-cast 3μ-ISD films is as large as possible.

Another feature of 3μ-ISD is that the interfaces between the PDMS and the PS microphases are darker than either of these two microphases (Figure 1a). This result suggests that some PI chains might be sitting on the interface between the PDMS and PS. Such an arrangement may be possible for ABC 3-miktoarm star terpolymer because three chains are connected by single junctions, which are not located on the interface between the PDMS and the PS microphases. One of the possible reasons accounting for this phenomenon is that the PI chains intervene between the PDMS and the PS microphases to prevent the strongest repulsive interaction between PDMS and PS. In addition, the PI content is relatively too large (1:0.8:0.85) to allow the tetragonal packing of polyhedral columns (Figure 1b), as predicted by Dotera et al.[25,26] (1:0.37−0.7:1). Therefore, an extra

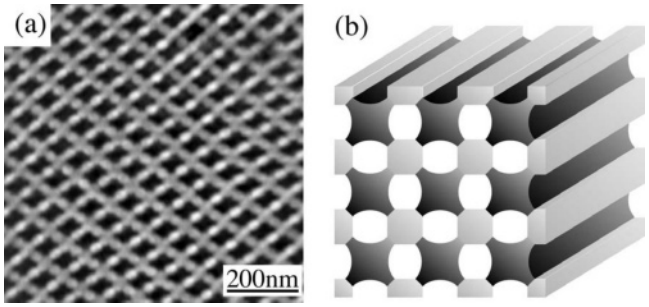

Figure 3. (a) TEM image of 3μ-ISD-2D stained with OsO_4. (b) Schematic illustration of the model for the microdomain structure of 3μ-ISDs consisting of dark (PI), gray (PDMS), and bright (PS) cylinders.

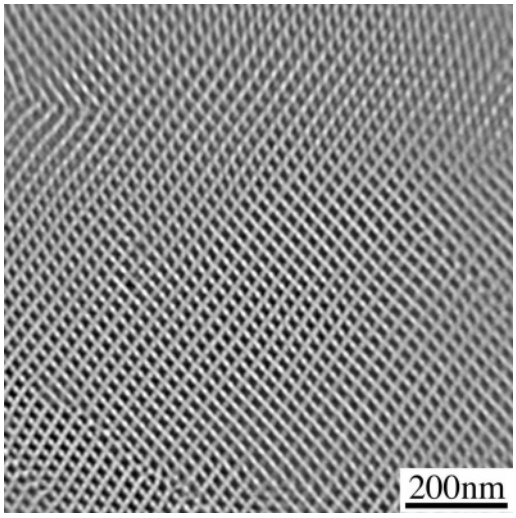

Figure 4. Low-magnification TEM image of 3μ-ISD-2D stained with OsO_4.

PI component must have invaded the interface between the PDMS and the PS to adjust the packing of the cylinders. The fastest and simplest method to approach Dotera's ratio is blending the star with the corresponding homopolymers. Thus, 3μ-ISD-2D was prepared by blending PDMS homopolymer with 3μ-ISD in the following ratio: 1.00:0.80:0.99 (Table 1). The TEM image of the as-cast film of 3μ-ISD-2D from toluene solution after OsO_4 staining is shown in Figure 3a. Although the symmetry of the microdomain structure packed in a square lattice did not change, the dark lines suggesting the invasion of the PI component into the interstices between the PS and the PDMS microdomains as observed in Figure 1a have disappeared in Figure 3a. This result suggests that the PDMS homopolymer must have entered the PDMS cylindrical domains and compensated for the shortage of the PDMS content to afford the optimum composition for tetragonal symmetry.

The microdomain structure of 3μ-ISD blended with PDMS homopolymer is dramatically different not only on the nanometer scale (Figure 3a) but also on the micrometer scale as shown by the low-magnification TEM image of 3μ-ISD-2D (Figure 4). Surprisingly, the 3μ-ISD-2D grain size became extremely large compared with that of neat 3μ-ISD. The irregular microdomain structures observed in the major area of neat 3μ-ISD were not present in the 3μ-ISD-2D images. The improvement in grain sizes by the addition of a small amount of homopolymers is often observed for linear block copolymers as well. Moreover, a 3D reconstructed image of 3μ-ISD-2D by electron tomography revealed

that the three kinds of cylindrical structures are straight (Figure 3b) and not curved into an arc (Figure 1b). The results of the electron tomography study of 3μ-ISD blended with PDMS homopolymer will be described elsewhere.[47]

It seems that the addition of a small amount of PDMS homopolymers with a molecular weight (1.3 kg mol^{-1}) lower than that of the PDMS arm (19.0 kg mol^{-1}) chain of 3μ-ISD remarkably increased the grain size. Because grain size is one of the criteria for microdomain stability, it is clear that the composition of 3μ-ISD-2D is in the suitable range to allow the packing of cylinders in a square lattice (Figure 4). In addition, macrophase separation between 3μ-ISD and the PDMS homopolymer was not observed, meaning that the PDMS homopolymer was incorporated into the 3μ-ISD PDMS microphases. These results imply that the volume ratio of the three components is a key factor for ordering the microdomain structure in 3μ-ABC. To determine if there is another stable microdomain structure, we added more PDMS homopolymer to 3μ-ISD to prepare 3μ-ISD-3D and 3μ-ISD-4D blends with PI/PS/PDMS volume ratios of 1.00:0.80:1.23 and 1.00:0.80:2.00, respectively. The TEM images of 3μ-ISD-3D and 3μ-ISD-4D together with those of neat 3μ-ISD and 3μ-ISD-2D are provided in Figures 5. Surprisingly, the tetragonal symmetry of the microdomain structures was not altered in any of these samples, despite the large differences in their PDMS homopolymer volume fraction (Table 1). The grains in 3μ-ISD-3D and 3μ-ISD-4D are as large as those in 3μ-ISD-2D. In addition, macrophase separation between 3μ-ISD and the PDMS homopolymer was not observed.

As stated above, the optimum volume ratio for the tetragonal pattern is very close to that of 3μ-ISD-2D (1.00:0.84:0.99). The tetragonal patterns in the three samples seem to be maintained even if the PDMS volume fraction rises dramatically, indicating that only part of the PDMS must be incorporated into the cylindrical PDMS microdomains (Figure 5c and d, respectively). The excess PDMS must be excluded from the PDMS cylinders and relocated elsewhere. If we change the PDMS volume fraction by preparing a star with a longer PDMS arm, then the symmetry of the microdomain structure should change accordingly because the PDMS chains are connected to the PI and PS chains by the single junction points confined on lines where the three interfaces (PI/PS, PS/PDMS, and PDMS/PI) meet. In contrast, in the case where PDMS homopolymer is added to 3μ-ISD, the PDMS homopolymer chain is free to choose its locations and is not necessarily introduced into the PDMS microdomains. However, the PDMS arm chains are tethered from the line where the three interfaces meet and always contribute to the formation of the PDMS microdomains. Because the microdomain structure did not change upon addition of the PDMS homopolymer, we can assume that the cylindrical microdomain structure with tetragonal symmetry is inherent to 3μ-ISD and cannot be altered without changing the composition of the 3-miktoarm star terpolymer itself.

The observations above lead to the question of the location of the excess homopolymer in 3μ-ISD-3D and 3μ-ISD-4D. Evidence of the localization of the PDMS homopolymer is particularly strong in 3μ-ISD-4D. TEM images of some areas in 3μ-ISD-4D are provided in Figure 6. Similar defects were also observed in 3μ-ISD-3D but less frequently. It is quite difficult to determine

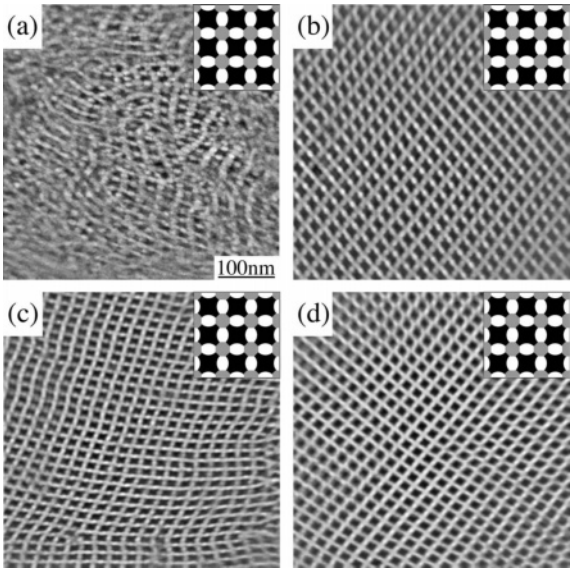

Figure 5. TEM images of 3μ-ISD and its blends with the PDMS homopolymer (3μ-ISD-2D−3μ-ISD-4D): (a) 3μ-ISD, (b) 3μ-ISD-2D, (c) 3μ-ISD-3D, and (d) 3μ-ISD-4D. All samples were stained with OsO_4. The inset images are the schematic models of the cross-sectional views of cylindrical microdomains for the corresponding samples. The same scale bar as shown in a applies for b−d.

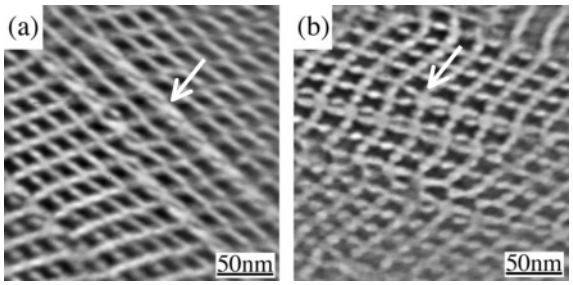

Figure 6. TEM images of the defects (indicated by the white arrows) in 3μ-ISD-4D stained with OsO_4.

the exact shapes of these defects from the TEM images. However, it is clear that the PDMS microphase size in the defects is apparently larger than that in the corresponding regular structure with tetragonal symmetry. Therefore, we can conclude that the excess PDMS homopolymer is located in the PDMS microdomains in the defect areas (Figure 6). However, the PDMS/PS volume ratio is almost 2 in 3μ-ISD-4D (Table 1), whereas the PDMS/PI volume ratio as estimated from the corresponding areas in the TEM images in Figure 6 is less than 2. Although not corroborated by our TEM observation, the excess PDMS homopolymer could be macrophase-separated from the terpolymer to form large homopolymer domains.

It should be emphasized that the line defects observed in 3μ-ISD 3 and 4 present interesting industrial applications such as waveguides in photonic crystals. These line defects increased upon increasing the amount of PDMS homopolymer, but in order to be useful, this phenomenon must be predicted and controlled.

It should be mentioned that Lu et al.[48] theoretically treated the effect of mixing the ABC 3-miktoarm star terpolymers with homopolymers by computer simulation with dynamic density fluctuation theory and clearly observed changes in the microdomain morphology with homopolymer content. Their results contradict our observations of the real system; however, the compari-

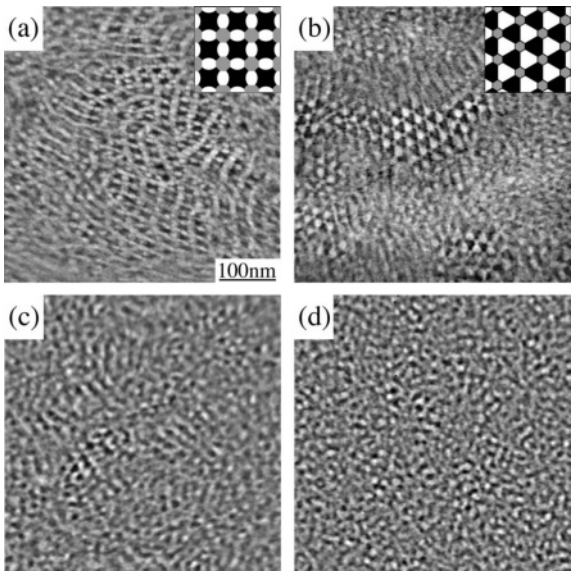

Figure 7. TEM images of 3μ-ISD and its blends with the PS homopolymer (3μ-ISD-5S−3μ-ISD-7S): (a) 3μ-ISD, (b) 3μ-ISD-5S, (c) 3μ-ISD-6S, and (d) 3μ-ISD-7S. All samples were stained with OsO_4. The inset images are the schematic models of the cross-sectional views of cylindrical microdomains for the corresponding samples. The same scale bar as shown in a applies for b−d.

son is difficult because of the large differences in molecular parameters and experimental conditions.

We also investigated the effect of blending PS homopolymer (2.8 kg mol^{-1}) with 3μ-ISD (Table 1). The TEM image of 3μ-ISD-5S, for which the PI/PS/PDMS volume ratio was adjusted by blending PS homopolymer to 1.00:1.00:0.84, is given in Figure 7b. This composition is similar to that of 3μ-ISD-2D, with the PS and PDMS values interchanged. Thus, tetragonal symmetry with PS and PDMS microdomains interchanged is expected if we neglect the asymmetric interaction among the three components. However, this change caused the transformation from tetragonal to hexagonal symmetry (Figure 7b). The asymmetric interaction could be responsible for the change in symmetry in order to maintain the minimum interfacial area between PS and PDMS. The small difference in the volume fraction of the minor component between 3μ-ISD-2D (PS: 0.287) and 3μ-ISD-5S (PDMS: 0.296) could not be responsible for this because a further increase in PS content did not produce tetragonal symmetry (Figure 7c and d). The largest 3μ-ISD-5S grain size is only ~100 nm and is smaller than either that of 3μ-ISD-2D or 3μ-ISD. The above result suggests that the hexagonal symmetry in 3μ-ISD-5S may not be stable.

As in the case of PDMS homopolymer blends, more PS homopolymer was added to 3μ-ISD to afford 3μ-ISD-6S and 3μ-ISD-7S, with PI/PS/PDMS volume ratios of 1.00:1.13:0.84 and 1.00:1.46:0.84, respectively. TEM images of 3μ-ISD-6S and 3μ-ISD-7S are given in Figure 7c and d, respectively (Table 1). A small difference in the amount of PS homopolymer added changed the microdomain morphologies dramatically, but in the opposite direction than in the case of the PDMS homopolymer blends (Figure 7c and d). From this Figure, it is clear that there is no regular microdomain structure, suggesting that the hexagonal symmetry is not stable and hence disappears upon further addition of PS homopolymer.

From the results above, it seems that blending with PS does not alter characteristic features (small grain size and bent cylinder morphology) of the neat 3μ-ISD. Combining these results with those of our previous study,[22] we consider that the inherent 3μ-ISD composition is not an appropriate one for the tetragonal array of three kinds of cylinders, even though it is the most favorable microdomain structure for neat 3μ-ISD. Thus, 3μ-ISD tends to form a tetragonal array of cylinders, but the cylinders start to bend because the volume fraction of each cylinder is not optimum for filling the space the arm chains with one end attached to the lines where the three kinds of interfaces meet are subject to strong frustration/tension due to the restricted space. Therefore, the regular microdomain array cannot extend for a long distance and is thus surrounded by irregular microdomains. Such a hypothesis leads to the conclusion that the composition and the asymmetric interaction are the major factors that determine the microdomain structure pattern symmetry in 3μ-ISD, as shown in Figure 1. The geometrical pattern of microdomain morphology depends on the composition; however, the relative interaction between two components affects the interfacial area. Consequently, to create morphology with different symmetry, 3μ-ISDs with different compositions should be prepared.

Nevertheless, we found that blending with a small quantity of PDMS leads to the formation of very large grains, which are very important for nanotechnology applications.

4. Conclusions

In conclusion, blending a neat 3-miktoarm star terpolymer of isoprene (I), styrene (S), and dimethylsiloxane (D), 3μ-ISD, with PDMS homopolymer having a lower molecular weight than that of the PDMS block leads to a large grain size without altering the tetragonal symmetry of the neat star. It seems that the added PDMS is inserted into the PDMS phase, straightening the bent cylinders and increasing the long-range order. However, blending with PS homopolymer leads to unstable hexagonal symmetry and grain sizes smaller than those of the neat star. It appears that in order to obtain another equilibrium symmetry it is necessary to modify the composition or the chemistry of the components of the neat star. Thus, the morphology of miktoarm stars is directed by the inherent chemical architecture of the molecule. Additional experimental results are necessary to better understand and control the self-assembly of miktoarm stars.

Acknowledgment. This work was supported in part by a Grant-in-Aid for Scientific Research (under grant nos. 17105004(S) and 14350497(B)) from the Japan Society for the Promotion of Science and in part by the 21st century COE program COE for a United Approach to New Materials Science. We thank Vasilios Bellas for his help in the preparation of the sample. The financial support of the Research Committee of the University of Athens is gratefully acknowledged by H.I. and N.H.

References and Notes

(1) Riess, G.; Schlienger, M.; Marti, S. *J. Macromol. Sci., Part B* **1980**, *17*, 355.
(2) Shibayama, T.; Hasegawa, H.; Hashimoto, T.; Kawai, H. *Macromolecules* **1982**, *15*, 274.
(3) Kudose, I.; Kotaka, T. *Macromolecules* **1981**, *7*, 2325.

(4) Mogi, Y.; Kotsuji, H.; Kaneko, Y.; Mori, K.; Matsushita, Y.; Noda, I. *Macromolecules* **1992**, *25*, 5408.
(5) Mogi, Y.; Mori, K.; Matsushita, Y.; Noda, I. *Macromolecules* **1992**, *25*, 5412.
(6) Stadler, R.; Auschra, C.; Beckmann, J.; Krappe, U.; Voigt-Martin, I.; Leibler, L. *Macromolecules* **1995**, *28*, 3080.
(7) Breiner, U.; Krappe, U.; Thomas, E. L.; Stadler, R. *Macromolecules* **1998**, *31*, 135.
(8) Bates, F. S.; Fredrickson, G. H. *Phys. Today* **1999**, *52*, 32.
(9) Birshtein, T. M.; Zhulina, E. B.; Polotsky, A. A.; Abetz, V.; Stadler, R. *Macromol. Theory Simul.* **1999**, *8*, 151.
(10) Goldacker, T.; Abetz, V.; Stadler, R.; Erukhimovich, I. Y.; Leibler, L. *Nature* **1999**, *398*, 137.
(11) Tanaka, Y.; Hasegawa, H.; Hashimoto, T.; Ribbe, A.; Sugiyama, K.; Hirao, A.; Nakahama, S. *Polymer J*. **1999**, *31*, 989.
(12) Goldacker, T.; Abetz, V. *Macromol. Rapid Commun*. **1999**, *20*, 415.
(13) Abetz, V.; Goldacker, T. *Macromol. Rapid Commun*. **2000**, *21*, 16.
(14) Goldacker, T.; Abetz, V.; Stadler, R. *Macromol. Symp.* **2000**, *149*, 93.
(15) Elbs, H.; Drummer, C.; Abetz, V.; Krausch, G. *Macromolecules* **2002**, *35*, 5570
(16) Hashimoto, T.; Yamauchi, K.; Yamaguchi, D.; Hasegawa, H. *Macromol. Symp.* **2003**, *201*, 65.
(17) Hadjichristidis, N.; Iatrou, H.; Behal, S. K.; Chludzinski, J. J.; Disko, M. M.; Garner, R. T.; Liang, K. S.; Lohse, D. J.; Milner, S. T. *Macromolecules* **1993**, *26*, 5812.
(18) Okamoto, S.; Hasegawa, H.; Hashimoto, T.; Fujimoto, T.; Zhang, H.; Kazama, T.; Takano, A.; Isono, Y. *Polymer* **1997**, *38*, 5275.
(19) Sioula, S.; Hadjichristidis, N.; Thomas, E. L. *Macromolecules* **1998**, *31*, 5272.
(20) Sioula, S.; Hadjichristidis, N.; Thomas, E. L. *Macromolecules* **1998**, *31*, 8429.
(21) Hückstädt, H.; Göpfert, A.; Abetz, V. *Macromol. Chem. Phys.* **2000**, *201*, 296.
(22) Yamauchi, K.; Takahashi, K.; Hasegawa, H.; Iatrou, H.; Hadjichristidis, N.; Kaneko, T.; Nishikawa, Y.; Jinnai, H.; Matsui, T.; Nishioka, H.; Shimizu, M.; Furukawa, H. *Macromolecules* **2003**, *36*, 6962.
(23) Takahashi, K.; Hasegawa, H.; Hashimoto, T.; Bellas, V.; Iatrou, H.; Hadjichristidis, N. *Macromolecules* **2002**, *35*, 4859.
(24) Takano, A.; Soga, K.; Asari, T.; Suzuki, J.; Arai, S.; Saka, H.; Matsushita, Y. *Macromolecules* **2003**, *36*, 8216.
(25) Dotera, T. *Phys. Rev. Lett.* **1999**, *82*, 105.
(26) Gemma, T.; Hatano, A.; Dotera, T. *Macromolecules* **2002**, *35*, 3225.
(27) Tse, M. F. *J. Adhes. Sci. Technol*. **1989**, *3*, 551.
(28) Tse, M. F. *J. Adhes.* **1995**, *48*, 149.
(29) Tse, M. F.; Jacob, L. *J. Adhes.* **1996**, *56*, 1996.
(30) Deng, T.; Chen, C.; Honeker, C.; Thomas, E. L. *Polymer* **2003**, *44*, 6549.
(31) Cheng, J. Y.; Ross, C. A.; Chen, V. Z. H.; Thomas, E. L.; Lammertink, R. G. H.; Vancso, G. J. *Adv. Mater.* **2001**, *13*, 1174.
(32) Naito, K.; Hieda, H.; Sakurai, M.; Kamata, Y.; Asakawa, K. *IEEE Trans. Magn.* **2002**, *38*, 1949.
(33) Lazzari, M.; López-Quintela, M. A. *Adv. Mater.* **2003**, *15*, 1583.
(34) Kim, S. O.; Solak, H. H.; Stoykovich, M. P.; Ferrier, N. J.; de Pablo, J. J.; Nealey, P. F. *Nature* **2003**, *424*, 14.
(35) Green, P. F.; Christensen, T. M.; Russell, T. P.; Jérôme, R. *Macromolecules* **1989**, *22*, 2189.
(36) Russell, T. P.; Coulon, G.; Deline, V. R.; Miller, D. C. *Macromolecules* **1989**, *22*, 4600.
(37) Coulon, G.; Ausserre, D.; Russell, T. P. *J. Phys.* **1990**, *51*, 777.
(38) Amundson, K.; Helfand, E.; Davis, D. D.; Quan, X.; Patel, S. S.; Smith, S. D. *Macromolecules* **1987**, *20*, 1651.
(39) Ferri, D.; Wolff, D.; Springer, J.; Francescangeli, O.; Laus, M.; Angeloni, A. S.; Galli, G.; Chilellini, E. *J. Polym. Sci., Part B: Polym. Phys.* **1998**, *36*, 21.
(40) Winter, H. H.; Scott, D. B.; Gronski, W.; Okamoto, S.; Hashimoto, T. *Macromolecules* **1993**, *26*, 7236.
(41) Chen, Z. R.; Issaian, A. M.; Kornfield, J. A.; Smith, S. D.; Grothaus, J. T.; Satkowski, M. M. *Macromolecules* **1997**, *30*, 7096.
(42) Hashimoto, T.; Bodycomb, J.; Funaki, Y.; Kimishima, K. *Macromolecules* **1999**, *32*, 952.
(43) Bodycomb, J.; Funaki, Y.; Kimishima, K.; Hashimoto, T. *Macromolecules* **1999**, *32*, 2075.
(44) Bellas, V.; Iatrou, H.; Hadjichristidis, N. *Macromolecules* **2000**, *33*, 6993.
(45) Yamauchi, K.; Akasaka, S.; Hasegawa, H.; Hashimoto, T.; Iwawaki, E.; Masuda, T. *Macromolecules*, to be submitted for publication.
(46) Hashimoto, T.; Mori, K.; Hasegawa, H. *Polymer* **1990**, *31*, 2368.
(47) Yamauchi, K. et al., to be submitted for publication.
(48) Lu, T.; He, X.; Liang, H. *J. Chem. Phys.* **2004**, *12*, 9702.

MA050716K